A Multivariable Controller for the Start-up Procedure of a Solar Membrane Distillation Facility

Juan D. Gil * **Lidia Roca** ** **Manuel Berenguel** *
José Luis Guzmán *

* *Centro Mixto CIESOL, ceiA3, Universidad de Almería. Ctra. Sacramento s/n, Almería 04120, Spain; {juandiego.gil,beren,joseluis.guzman}@ual.es.*
** *CIEMAT-Plataforma Solar de Almería, Ctra. de Senés s/n, Tabernas 04200, Almería, Spain; {lidia.roca}@psa.es*

Abstract: This paper presents a multivariable TITO (two inputs two ouputs) controller aimed to improve the start-up procedure of a Solar Membrane Distillation (SMD) facility, located at Plataforma Solar de Almería (PSA). The control structure includes PID controllers and decouplers, as well as a reference governor based on a real time optimizer. The filtered Smith Predictor (SP) control structure has been used for controlling one of the output variables, whereas a cascade control scheme is employed to control the other one. The proposed approach has been tested in simulation on a nonlinear model of the SMD facility, showing promising results.

Keywords: Process Control, Solar Thermal Energy, PID Controllers, Smith Predictor, Reference Governor.

1. INTRODUCTION

SMD is an under-investigation thermal desalination technology that uses solar energy as source (Zaragoza et al., 2014; Cipollina et al., 2012). The use of solar energy allows membrane distillation technology to be an efficient and a sustainable solution to mitigate the lack of water in places with good solar irradiance conditions and access to brackish or sea water. However, due to its unpredictable nature, it requires the use of specific energy storage systems and suitable discontinuous operation techniques, which can be obtained by means of adequate control strategies (Gil et al., 2018a).

There exist few works in the literature related with the automatic control of SMD facilities. In (Chang et al., 2010), a control system based on ON/OFF controllers is proposed to attain the optimal operation points calculated by means of an offline optimization technique. This control approach was tested in simulation in a nonlinear dynamic SMD model. In the same way, in (Chang et al., 2012), ON/OFF controllers are employed to control the temperature difference between the output of the solar field and the buffering system. Another example is the one presented in (Lin et al., 2011), in which two control loops aimed at controlling the solar field temperature were tested in simulation. Nevertheless, as suggested in (Gil et al., 2018a), the key element for the successful combination of membrane distillation processes with solar energy is the use of low level controllers combined with real time optimizers, that take into consideration the plant conditions at each sample time. In this sense, a more complete control approach is the one proposed in (Karam and Laleg-Kirati, 2015), in which an optimal control algorithm was developed to regulate the feed flow rate according to the operating conditions, trying to maximize the distillate production. In (Porrazzo et al., 2013), a neural network model of the SMD facility was developed. Then, the neural network was used to set a feedforward optimal control system focused on maximizing the distillate production. In the previous work (Gil et al., 2018a), a hierarchical control system composed by two layer was proposed for the real time optimization of the plant operation, in terms of distillate production, thermal efficiency and cost savings.

This paper presents an improvement of the control approach proposed in (Gil et al., 2018a), by developing a new start-up procedure that allows to minimize the starting time of the membrane distillation module. This start-up procedure includes a multivariable TITO controller complemented with a real time optimizer-based reference governor. On the one hand, the reference governor generates the optimal setpoints for the multivariable controller at each sample time, using a static model of the SMD facility (Gil et al., 2018a). On the other hand, the multivariable control structure is formed by two PID-based controllers with feedforward and decouplers, which are in charge of tracking the optimal references calculated by the reference governor. The controlled variables are the inlet and outlet solar field temperatures. The outlet solar field temperature is controlled with a cascade control system, following the ideas presented in (Gil et al., 2018a,b). Con-

⋆ Research supported by the projects DPI2014-56364-C2-1/2-R (ENERPRO) and DPI2014-55932-C2-1-R (PROBIOREN) financed by the Spanish Ministry of Economy, Industry and Competitiveness and ERDF founds.

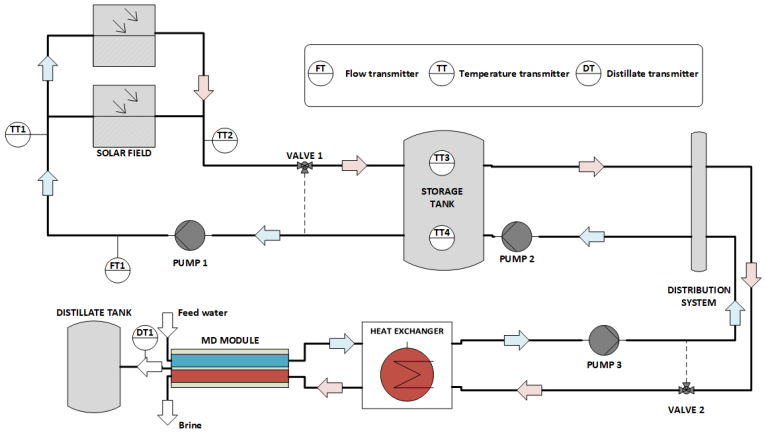

Fig. 1. Schematic diagram of the plant.

versely, a filtered SP control structure (Normey-Rico and Camacho, 2007) is used for controlling the inlet solar field temperature, in order to deal with the dominant time delay of the process. The proposed approach has been tested in simulation, using as real plant the nonlinear dynamic model of the SMD facility. Besides, a comparison with a typical manual operation is provided, evidencing the benefits obtained with the application of the control technique. Notice that the techniques used in this paper are widely known, and the contribution consists of applying these techniques to a real process, with the aim of reducing the time spent in its start-up procedure.

Table 1. Variables of interest for this work monitored in the SMD facility.

Variable	Description	Units
B1	Pump 1 frequency	%
DT1	Distillate production	L/min
FT1	Solar field water flow rate	L/min
I	Global irradiance measured at 36º tilted	W/m^2
T_a	Ambient temperature	^{o}C
TT1	Solar field inlet temperature	^{o}C
TT2	Solar field outlet temperature	^{o}C
TT3	Temperature at the top of the tank	^{o}C
TT4	Temperature at the bottom of the tank	^{o}C
V1	Valve aperture	%

2. SMD FACILITY

Fig. 1 shows the schematic diagram of the SMD facility at PSA. As can be observed, the membrane distillation unit is coupled with the heat generation circuit by means of its own heat exchanger, which is used for heating the sea feed water. Then, a distribution system is employed to connect the heat exchanger with the storage tank, which is used to balance transient or irradiance disturbances. Finally, the buffer system is connected directly with the thermal solar field, which is composed by flat-plate collectors. In (Zaragoza et al., 2014; Gil et al., 2018a) a complete description of the SMD plant was presented. It should be noted that other heating and cooling systems included in the facility are not considered in this work.

3. SYSTEM MODELING

In this section, the models of the main components involved in this work are presented. Notice that the full model of the heat generation circuit was developed in (Gil et al., 2018a,b), and the model of the membrane distillation unit was presented in (Ruiz-Aguirre et al., 2017).

Thus, the solar field outlet temperature is given by the following equations (Roca et al., 2009):

$$A_{sf} \cdot \rho \cdot c_p \cdot \frac{\partial \mathrm{TT2}(t)}{\partial t} = \beta \cdot \mathrm{I}(t) - \frac{H}{L_{eq}} \cdot (\bar{T}(t) - \mathrm{T}_a(t)) - c_p \cdot \dot{m}_{eq} \cdot \frac{\mathrm{TT2}(t) - \mathrm{TT1}(t)}{L_{eq}}, \tag{1}$$

where:

$$L_{eq} = L_a \cdot n_{cs}, \tag{2}$$

$$\dot{m}_{eq} = \frac{\mathrm{FT1}(t) \cdot \rho}{c_1}, \tag{3}$$

$$\bar{T}(t) = \frac{\mathrm{TT1}(t) + \mathrm{TT2}(t)}{2}, \tag{4}$$

A_{sf} is the collector cross section area (0.007 m^2), ρ is the water density (kg/m^3), c_p is the specific heat capacity of water (J/kg^{o}C), β is the irradiance model parameter (0.11 m), H is the solar field global thermal losses coefficient (5.88 J/(sK)), L_a is the collector absorver tube length (1.95 m), n_{cs} is the number of series-connections in a collectors group (5), and c_1 is a conversion factor used for taking into account connections, number of modules and L/min conversion ($9{\cdot}2{\cdot}6{\cdot}10^4$ s·L/min·m^3). The rest of variables are defined in Table 1.

On the other hand, the inlet solar field temperature is modeled with the static model of the mix produced in the three way mixing valve (see Valve 1 in Fig. 1), which is described by the following equation:

$$\mathrm{TT1}(t) = \mathrm{TT4}(t) \cdot (1 - \gamma) + \mathrm{TT2}(t) \cdot \gamma, \tag{5}$$

where γ is the valve aperture. In addition, a low pass filter with a representative time constant of 23 s has been added at the output of this static model in order to fit real data.

Finally, the flow-dependent delays (d_{TT_i}), produced by temperature transmitter ($\tilde{TT}_i$) locations, are computed

according to the procedure presented in Normey-Rico et al. (1998):

$$\mathrm{TT}_i(t) \approx \tilde{TT}_i(t - d_{\mathrm{TT}_i}), \tag{6}$$

$$L = \int_0^{d_{\mathrm{TT}_i}} v(t)dt \rightarrow L = \frac{T_s}{A}\sum_{i=0}^{n-1} f(k-1), \tag{7}$$

where v is the fluid velocity, T_s is the sample time, n is the delay as multiple of the sample time, A is the pipe cross section area, L is the length of the pipe, and $f(k)$ is the flow rate at discrete-time instant k.

4. CONTROL STRUCTURE DESIGN

As it has been mentioned previously, the objective is to develop a control structure aimed at improving the start-up procedure of the SMD plant. One of the main constraints when operating the membrane distillation module is its limited operating temperature range, between 60-80 °C. 80 °C is the maximun admissible temperature by membrane materials, while temperatures lower than 60 °C produce very little distillate. So, it is not economical profitable to operate the membrane distillation module below 60 °C. Thus, with the plant configuration presented in Section 2, at the beginning of the operation, the solar field must be used to increase the temperature of the tank, until reaching a temperature that allows to operate the membrane distillation module above 60 °C. In the manual operation, first, the fluid is only recirculated in the solar field (closing Valve 1). Then, when a high temperature at the output of the solar field is reached, such as 80 °C, Valve 1 is opened, and the fluid is recirculated trough the storage tank until its temperature is adequate to operate membrane distillation module above 60 °C, moment in which pump 2 is started. Nevertheless, this procedure takes long time and does not assure that the solar field outlet temperature is going to be higher than the temperature in the tank because, when Valve 1 is closed, the inlet temperature changes drastically. To solve these problems, in (Gil et al., 2018a) two improvements were included. Firstly, the steady-state solar field model was used to estimate the irradiance value required to turn the solar field on and to assure heating the tank. Secondly, a predictive controller was added to estimate the solar field temperature setpoints to maximize the temperaure in the tank. In this work, this methodology has been improved by using Valve 1 which allows reducing the time to heat the tank.

In the proposed method, Valve 1 is used to obtain an adequate temperature at the inlet of the solar field that guarantees an outlet temperature for heating the tank. It should be noted that, at the beginning of the operation, the fluid is recirculated only trough the solar field, with Valve 1 closed, and pump 1 at the minimum, providing a flow rate (FT1) of 7.5 L/min. Once the outlet solar field temperature reaches the tank top temperature, the control procedure starts. As can be observed in Fig. 2, the control structure is composed by a reference governor which generates the optimal references for a multivariable TITO controller, trying to maximize the thermal energy storage in the tank, ensuring, at each sample time, that the temperature of the fluid flowing to the tank is going to be higher than the one in the upper part of the tank. On the other hand, the multivariable controller is in charge of controlling the inlet solar field temperature by means of the mix produced in Valve 1 (see Fig. 1), and the outlet solar field temperature by using pump 1. Thus, the tank can be loaded when low values of global irradiance are available, reaching the temperature necessary to operate the membrane distillation module faster. In the following subsections the control structure design is presented.

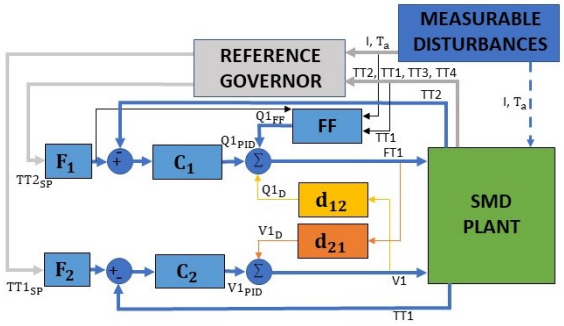

Fig. 2. Control scheme. F_1 and F_2 are reference filters, C_1 and C_2 are PID-based controllers, and d_{12} and d_{21} are decouplers.

4.1 Reference governor

As has be mentioned before, the main objective of the reference governor is to provide optimal references for the multivarible controller, trying to maximize the thermal energy storage in the tank. To do this, as was established in Gil et al. (2018a), the outlet solar field temperature should be as close as possible to the one at the top of the tank.

Hence, the reference governor uses the static model of the solar field and the mix produced in Valve 1 to calculate the optimal references ($\mathrm{TT2_{SP}}$ and $\mathrm{TT1_{SP}}$). The optimization problem to be solved in the reference governor at each sample time is described by the following equations, where for the sake of simplicity, variables without explicit dependence on discrete time (k) are also time dependent but estimated using static models and measured variables (those using explicit dependence on k):

$$\min_{\gamma, FT1} J = \mathrm{TT2} - \mathrm{TT3}(k) \tag{8}$$

subjected to:

$$\mathrm{TT2} = \mathrm{TT1} + \left[\beta \cdot L_{eq} \cdot \mathrm{I}(k) - H \cdot (\bar{T} - \mathrm{T}_a(k))\right] \cdot \frac{c_1}{\mathrm{FT1} \cdot c_p \cdot \rho}, \tag{9}$$

$$\bar{T} = \frac{\mathrm{TT2} + \mathrm{TT1}}{2} \tag{10}$$

$$\mathrm{TT1} = \mathrm{TT4}(k) \cdot (1 - \gamma) + \mathrm{TT2} \cdot \gamma, \tag{11}$$

$$\mathrm{TT2_{min}} \leq \mathrm{TT2} \leq \mathrm{TT2_{max}}, \tag{12}$$

$$\mathrm{TT3}(k) \leq \mathrm{TT2}, \tag{13}$$

where J is the objective function to be minimized, $\mathrm{TT2_{min}}$ and $\mathrm{TT2_{max}}$ are the maximum and minimum temperatures reachable at the outlet of the solar field, calculated

with the static model of the solar field (Eq. (9)) with FT1 equal to 20 and 7.5 L/min respectively. Notice that the decision variables of the optimization problem are γ and FT1, so then, the optimal references ($TT2_{SP}$ and $TT1_{SP}$) are calculated with the static models presented in Eq. (9) and (11) respectively. Although the control signal obtained by the optimization method can be applied directly to the plant, this usually causes abrupt control actions, obtaining undesired responses. In this way, the temperature references are calculated and the multivariable controller tries to track them, obtaining smooth responses and control actions. It should be also commented that current values of TT3(k) and TT4(k) are used in the optimization problem instead of estimated ones since they do not suffer significant changes along the sample time adopted.

4.2 Multivariable controller

This section presents the development of the multivariable TITO controller. In this problem, the two inputs are the Valve 1 aperture (γ) and the solar field flow rate (FT1), and the outputs are the inlet and the outlet solar field temperature (TT1 and TT2). The modeling, the pairing of variables, and the study of the coupling between variables are presented below.

Modeling and pairing of variables The first step consists on modeling the relationship between input and output variables. Open-loop tests have been carried out in the real facility at PSA, introducing typical step changes in the input variables. Then, the reaction curve method has been used to obtain the relation between input and output variables, in the form of first order plus dead time (FOPDT) transfer function $G(s) = Y(s)/U(s) = k \cdot e^{L_n \cdot s}/(\tau s + 1)$, where k is the static gain, τ is the representative time constant and L_n is the nominal dead time. The relationship matrix is given by:

$$[\mathbf{Y}] = [\mathbf{G}] \cdot [\mathbf{U}], \tag{14}$$

$$\begin{pmatrix} Y_1 \\ Y_2 \end{pmatrix} = \begin{pmatrix} \frac{-1.37}{66.62s+1}e^{-16s} & \frac{0.09}{75s+1}e^{-120s} \\ \frac{-0.26}{330s+1}e^{-280s} & \frac{0.102}{28s+1}e^{-79s} \end{pmatrix} \cdot \begin{pmatrix} U_1 \\ U_2 \end{pmatrix}, \tag{15}$$

where Y_1 and Y_2 are TT2 and TT1 respectively, and U_1 and U_2 are FT1 and γ respectively.

Once the relation between variables have been obtained, the pairing of variables must be established. To evaluate the interactions between variables the relative gain array (RGA) analysis has been used. The RGA matrix of the system at hand is given by:

$$\Lambda = \begin{pmatrix} 1.20 & -0.20 \\ -0.20 & 1.20 \end{pmatrix}, \tag{16}$$

and according to this result, the pairing of variables must be: 1) Y_1 with U_1 (TT2 with FT1), and 2) Y_2 with U_2 (TT1 with γ), as was to be expected from the layout of the system.

PID controllers design The second step to develop the multivariable controller consists on the PID-based controllers design. As the interaction between variables is not too strong (see RGA matrix, Eq. (16)), the PID-based controllers can be tuned separately.

Firstly, to control the outlet solar field temperature (TT2), a cascade controller (C_1 in Fig. 2) is used. The slave controller is in charge of providing the desired flow rate (FT1) by manipulating the pump 1, whereas the outer loop chooses the flow rate for controlling TT2. Besides, a feedforward based on the static model of the solar field (FF in Fig. 2) is used to improve the disturbance rejection. The development of this control loop has been already presented in Gil et al. (2018a,b). Several tuning methods have been tested in simulation, e.g. (Moliner and Tanda, 2016), and finally those stated in the caption of Table 2 (where the tuned parameters of the controllers are shown) have been used.

Table 2. PID configurations using the Ideal PID transfer function. T_r is the characteristic time constant of the first order reference filter, and T_f is the characteristic time constant of the first order filtered SP controller. The first controller has been tuned using the AMIGO method (Åström and Hägglund, 2005), the second controller using the SIMC method (Skogestad, 2003), and the third one using the cancellation polo-cero method (Åström and Hägglund, 2005).

Controller	**Controlled variable**	**K_c**	**T_i(s)**	**T_r(s)**	**T_f(s)**
C_1	FT1	2.84 ((%·min)/L)	4.92	-	-
C_1	TT2	-0.42 (L/(min·°C))	72.60	34	-
C_2	TT1	0.06 (%/°C)	1.08	43	39.50

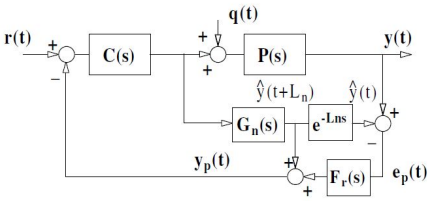

Fig. 3. Filtered Smith Predictor control structure (Normey-Rico and Camacho, 2007).

Secondly, as mentioned previously, the inlet solar field temperature is controlled with valve 1. As can be observed in the transfer function matrix (Eq. (15)), term G_{22}, the dead time of the process is dominant (normalized time delay of 0.73). Despite a simple PID-based control loop can be used to control the process, applying techniques as the ones presented in (Normey-Rico and Guzmán, 2013), when the dead time is dominant as the one presented in this problem, the performance of the system may deteriorate. Thus, additional solutions as the Smith Predictor (SP) should be taken into account for controller C_2 (Normey-Rico and Camacho, 2007). Nevertheless, it should be considered that modeling dead time errors, as the one presented in this problem due to variability of the flow rate (minimum dead time observed 67 s and maximum dead time observed 91 s), can drive SP control structure to degraded performance and even instability. In this way, the filtered SP structure (Normey-Rico and Camacho, 2007) can be used, adding robustness to the control

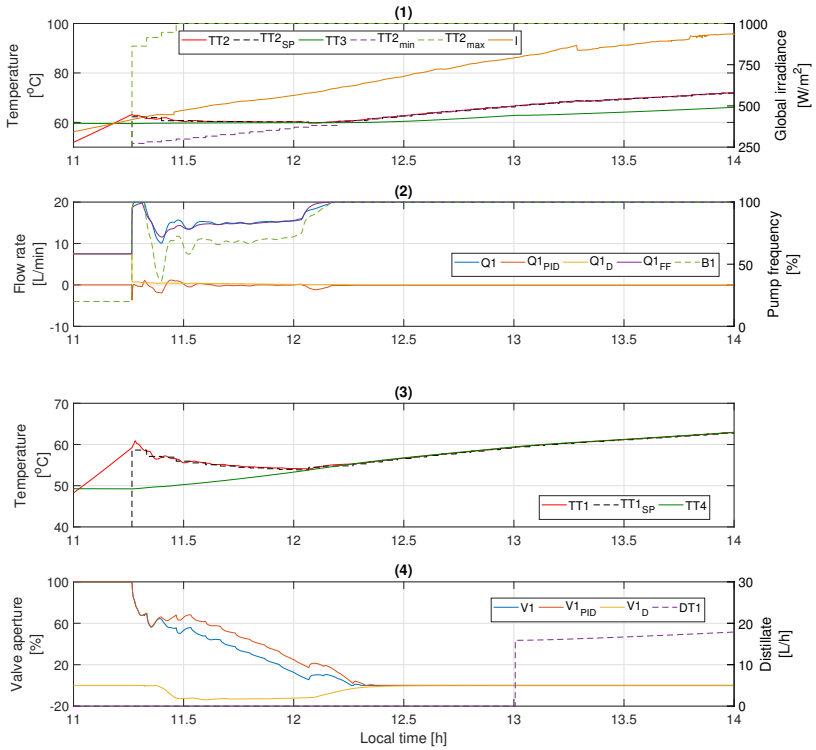

Fig. 4. Simulation results. PID suffixes refer to the PID controller actions, D suffixes refer to decoupler control signals, and FF suffix refers to feedforward control action.

solution (see Fig. 3). It should be also commented that the representative time constant of the filtered SP structure is calculated as T_f=0.5·L_n, following the ideas presented in (Normey-Rico and Camacho, 2007). Finally, the PI controller parameters are presented in Table 2. Notice that in this case, as in the cascade controller case, a reference first order filter has been added in order to obtain the desired closed-loop responses.

Decouplers The last step to develop the multivariable controllers is the configuration of decouplers. Although the use of decouplers is not essential in this work, as the interactions are not too strong (see Eq. (16)), they have been included in the control structure in order to improve the control action. It should be taken into account that, when using a SP structure, disturbance rejection cannot be faster than the open loop one (Normey-Rico and Camacho, 2007), so decouplers can help to obtain better disturbance rejection in terms of interaction between variables. The decoupler matrix is given by (Morilla et al., 2013):

$$D(s) = \begin{pmatrix} 1 & -\frac{G_{12}}{G_{11}} \\ -\frac{G_{21}}{G_{22}} & 1 \end{pmatrix} = \begin{pmatrix} 1 & \frac{0.09}{1.37}\frac{66.62s+1}{75s+1}e^{-104s} \\ \frac{0.26}{0.10}\frac{28s+1}{330s+1}e^{-201s} & 1 \end{pmatrix} \quad (17)$$

5. RESULTS AND DISCUSSION

The developed control structure has been tested in simulation in the nonlinear model of the SMD facility (see Section 3), using real data from PSA on the 10th March 2017. The sample time employed in the reference governor is 4 min, which has been choseen taking into account the closed loop representative time constant of each loop (around 120 s for the outlet solar field temperature control loop, and 170 s for the inlet solar field temperature one). On the other hand, the sample time of the multivariable controller is 1 s, according to the one employed in (Gil et al., 2018a,b).

At the beginning of the operation, the tank bottom temperature (TT4) is 50.2 ºC whereas the top tank temperature (TT3) is 60.4 ºC. Notice that real initial conditions of the plant have been used. As can be seen in Fig. 4, the operation starts in manual mode, as was mentioned in Section 4 , with FT1 equal to 7.5 L/min and V1 equal to 100 %, recirculating the fluid completely trough the solar field. Then, when the outlet solar field temperature is higher than the one at the top of the tank, time moment 11.15 h (see Fig. 4-1), the automatic operation begins. As can be observed in Fig. 4-1, the reference governor maintains $TT2_{SP}$ as close as possible to TT3 from 11.15 to 12.10 h. Later, from 12.10 h, the reference governor provides $TT2_{SP}$ close to the minimum temperature reachable. Fig. 4-2 shows how the flow rate is regulated by the multivariable controller to attain the temperature setpoints calculated by the reference governor. Besides, it can be observed that, from 11.15 to 12.10 h, the flow rate is increased continuously, according to the setpoints generated by the reference governor, until reaching the maximum (20 L/min) at time moment 12.10 h, increasing the thermal energy delivered to the tank in the same way. It should be noted that most of the control action is provided by the feedforward ($Q1_{FF}$) as it provides the

nominal flow rate according to the operating conditions and $TT2_{SP}$, whereas the contribution of the decoupler (d_{12} in Fig. 4) is low. In this loop, the steady state error is 0.13 °C and the overshoots are less than 5 %. On the other hand, Fig. 4-3 and 4-4 show the inlet solar field control loop performance. As can be observed, the reference governor generates setpoints for TT1 which allow TT2 to be as close as possible to TT3. Fig. 4-4 shows how the valve is opening gradually from 11.15 to 12.10 h, until it is completely open. Notice that in this loop the contribution (see $V1_D$ in Fig. 4-4) of the decoupler (d_{21} in Fig. 4) is greater that in the previous case. In this case, the steady state error is 0.11 °C and overshoots are also lower than 5 %.

The results presented in Fig. 4 have been compared with a manual operation and with the operation obtained with the approach presented in (Gil et al., 2018a), using the same starting conditions. As can be observed in Fig. 4-4, the module starts at 13.00 h, while with the approach presented in (Gil et al., 2018a) the module starts at 13.14 h, and with the manual operation the module starts to operate at 13.29 h. This fact produces that the distillate production augments by 6 % in comparison with the manual operation. The distillate production at the end of the day with the automatic operation is 204.2 L, while the one of the manual mode is 191.94 L. Notice that the distillate production of the approach presented in (Gil et al., 2018a) is not compared since it has an optimization problem focus on maximizing the thermal efficiency and minimizing operating cots, so the comparison is not made under the same conditions. It should be taken into account that the plant employed in this work is a small test-bed facility. In industrial applications, the improvements achieved by means of the application of the proposed control system can be very relevant for the daily operation.

6. CONCLUSION

This work has addressed the development of a multivariable controller with reference governor for improving the start-up procedure of a solar membrane distillation facility. Simulation results show that the adoption of the proposed technique can improve the daily distillation production by 6 % in comparison with the manual operation.

Futures works will be aimed at testing the proposed control technique in the real facility, and also at improving the reference governor for taking into account disturbance forecasting methods.

REFERENCES

Åström, K.J. and Hägglund, T. (2005). Advanced PID control. ISA-The Instrumentation, Systems, and Automation Society. *Research Triangle Park, NC*, 27709.

Chang, H., Lyu, S.G., Tsai, C.M., Chen, Y.H., Cheng, T.W., and Chou, Y.H. (2012). Experimental and simulation study of a solar thermal driven membrane distillation desalination process. *Desalination*, 286, 400–411.

Chang, H., Wang, G.B., Chen, Y.H., Li, C.C., and Chang, C.L. (2010). Modeling and optimization of a solar driven membrane distillation desalination system. *Renewable Energy*, 35(12), 2714–2722.

Cipollina, A., Di Sparti, M., Tamburini, A., and Micale, G. (2012). Development of a membrane distillation module for solar energy seawater desalination. *Chemical Engineering Research and Design*, 90(12), 2101–2121.

Gil, J.D., Roca, L., Ruiz-Aguirre, A., Zaragoza, G., and Berenguel, M. (2018a). Optimal operation of a solar membrane distillation pilot plant via nonlinear model predictive control. *Computers & Chemical Engineering*, 109, 151–165.

Gil, J.D., Roca, L., Zaragoza, G., and Berenguel, M. (2018b). A feedback control system with reference governor for a solar membrane distillation pilot facility. *Renewable Energy*, 120, 536–549.

Karam, A.M. and Laleg-Kirati, T.M. (2015). Real time optimization of solar powered direct contact membrane distillation based on multivariable extremum seeking. In *Control Applications (CCA), 2015 IEEE Conference on*, 1618–1623. IEEE.

Lin, J.S., Chang, H., and Wang, G.B. (2011). Modelling and control of the solar powered membrane distillation system. In *AIChE Annual Meeting*. Minneapolis, MN, USA.

Moliner, R. and Tanda, R. (2016). Tool for robust tuning of PI/PID controllers with two degree of freedom. *Revista Iberoamericana de Automática e Informática industrial*, 13(1), 22–31.

Morilla, F., Garrido, J., and Vázquez, F. (2013). Control multivariable por desacoplo, "Multivariable control by decoupling". *Revista Iberoamericana de Automática e Informática industrial*, 10, 3–17.

Normey-Rico, J.E., Bordons, C., Berenguel, M., and Camacho, E.F. (1998). A robust adaptive dead-time compensator with application to a solar collector field. *IFAC Proceedings Volumes*, 31(19), 93–98.

Normey-Rico, J.E. and Camacho, E.F. (2007). *Control of dead-time processes*. Springer Science & Business Media.

Normey-Rico, J.E. and Guzmán, J.L. (2013). Unified pid tuning approach for stable, integrative, and unstable dead-time processes. *Industrial & Engineering Chemistry Research*, 52(47), 16811–16819.

Porrazzo, R., Cipollina, A., Galluzzo, M., and Micale, G. (2013). A neural network-based optimizing control system for a seawater-desalination solar-powered membrane distillation unit. *Computers & Chemical Engineering*, 54, 79–96.

Roca, L., Guzmán, J.L., Normey-Rico, J.E., Berenguel, M., and Yebra, L.J. (2009). Robust constrained predictive feedback linearization controller in a solar desalination plant collector field. *Control Engineering Practice*, 17(9), 1076–1088.

Ruiz-Aguirre, A., Andrés-Mañas, J., Fernández-Sevilla, J., and Zaragoza, G. (2017). Modeling and optimization of a commercial permeate gap spiral wound membrane distillation module for seawater desalination. *Desalination*, 419, 160–168.

Skogestad, S. (2003). Simple analytic rules for model reduction and PID controller tuning. *Journal of Process Control*, 13(4), 291–309.

Zaragoza, G., Ruiz-Aguirre, A., and Guillén-Burrieza, E. (2014). Efficiency in the use of solar thermal energy of small membrane desalination systems for decentralized water production. *Applied Energy*, 130, 491–499.